BILINGUAL PUBLISHING CO.
Pioneer of Global Academics Since 1984

Journal of Geological Research
https://ojs.bilpublishing.com/index.php/jgr-a

ARTICLE

Application of integrated formation evaluation and three-dimensional modeling in shale gas prospect identification

Jin Gao[1*] Zhe Cao[1,2] Guangdi Liu[1,2] Longmei Zhao[3] Lijun Du[1,4] Yuhua Kong[5]

1. College of Geosciences, China University of Petroleum, Beijing, 102249, China
2. State Key Laboratory of Petroleum Resources and Prospecting, China University of Petroleum, Beijing, 102249, China
3. China United Coalbed Methane National Engineering Research Center Corporation Limited, Beijing, 100095, China
4. Fuyu Oil Production Plant in Jilin Oilfield Company, PetroChina, Songyuan, 138000, China
5. PetroChina Xinjiang Oilfield Company, Karamay, 834000, China

ARTICLE INFO

Article history
Received: 4 November 2019
Accepted: 20 December 2019
Published Online: 31 December 2019

Keywords:
Shale gas
Prospect
Prospective interval
Badaowan Formation
Junggar Basin

ABSTRACT

Identifying the shale gas prospect is crucial for gas extraction from such reservoirs. Junggar Basin (in Northwest China) is widely considered to have high potential as a shale gas resource, and the Jurassic, the most significant gas source strata, is considered as prospective for shale gas exploration and development. This study evaluated the Lower Jurassic Badaowan Formation shale gas potential combined with geochemical, geological, and well logging data, and built a three-dimensional (3D) model to exhibit favorable shale gas prospects. In addition, methane sorption capacity was tested for verifying the prospects. The Badaowan shale had an average total organic carbon (TOC) content of 1.30 wt. % and vitrinite reflectance (Ro) ranging from 0.47% to 0.81% with dominated type III organic matter (OM). X-ray diffraction (XRD) analyses showed that mineral composition of Badaowan shale was fairly homogeneous and dominated by clay and brittle minerals. 67 wells were used to identify prospective shale intervals and to delineate the area of prospects. Consequently, three Badaowan shale gas prospects in the Junggar Basin were identified: the northwestern margin prospect, eastern Central Depression prospect and Wulungu Depression prospect. The middle interval of the northwestern margin prospect was considered to be the most favorable exploration target benefitted by wide distribution and high lateral continuity. Generally, methane sorption capacity of the Badaowan shale was comparable to that of the typical gas shales with similar TOC content, showing a feasible gas potential.

1. Introduction

In the recent years, the world's demand for natural gas has grown rapidly. Worldwide natural gas consumption was 120 trillion cubic feet (Tcf) in 2012, and it was expected to reach 203 Tcf in 2040 [1]. The growing demand for natural gas has aroused interest in shale gas exploration worldwide [2-10]. Natural gas produced from shale in the United States accounted for about 10% of natural gas production in 2012, and the ratio was expected to rise up to 35% in 2035 [4].According to a systematic assessment of shale gas resources conducted by Energy

**Corresponding Author:*
Jin Gao,
College of Geosciences, China University of Petroleum, Beijing, 102249, China;
Email: rongaojin@126.com

DOI: https://doi.org/10.30564/jgr.v1i3.1385

Information Administration [11], there was 7795 Tcf of technically recoverable shale gas resources worldwide, which was comparable to the amount of conventional natural gas resources. In China, potential organic-rich shales deposited in both marine and lacustrine environments and ranged from Precambrian to Tertiary. Shale gas resources has been estimated as abundant as 134×10^{12} m^3 (4745 Tcf) in place and 32×10^{12} m^3 (1115 Tcf) of technically recoverable [11].

Currently, the main method used to locate the shale gas prospects is to superimpose contoured maps of key parameters and to find the areas which can satisfy the minimum requirement of each parameter. This method is convenient to be applied, thus has been employed broadly. For instance, shale gas prospect in the Bendarch–Fort Worth Basin in United States was located by defining the shale with thickness of at least 100 ft (30 m) within a gas-generation window [12]. Rawsthorn [13] has assessed shale gas resources of 26 basins in onshore Australia and identified 19 shale gas plays. In such identification, prospect was defined by the contoured maps of key factors including thickness, thermal maturity, mineral composition, lateral continuity and organic matter abundant. Chen et al. [14] combined contoured maps of shale thickness and burial depth to predict the favorable areas for shale gas exploration of Lower Silurian Longmaxi shale in the southern Sichuan Basin of China. Yan et al. [15] superimposed contours of TOC content, thermal maturity (vitrinite reflectance), thickness and burial depth to predict the favorable zones for shale gas exploration in the upper Yangtze area of South China. Similarly, this method has also been applied to define the favorable areas for shale gas accumulation in other regions [16-20].

Geological and geochemical parameters for shale gas prospect identification can vary largely on both horizontal and vertical scales. For instance, the vertical variability in the organic richness can vary on relatively short vertical scales even less than 1 meter [21-24]. Similarly, thermal maturity also varies with burial depth. However, contour maps only display horizontal variation, cannot reflect this vertical variation, so the vertical distribution of organic-rich shales is difficult to determine from contour maps superimposition. As such, the use of superimposing contour maps alone is not necessarily precise for identifying shale gas prospects. Shale gas prospect is needed to be identified from a spatial perspective.

The Junggar Basin, one of the most important petroleum bearing basins in China, contained several source rocks that were initially estimated to have a large potential of unconventional shale gas resources [25-28]. Lower Jurassic Badaowan shale in the Junggar Basin was one of the most important gas source rocks. Several gas fields have been proven to be sourced by the Badaowan shale [29]. In 2011, a comprehensive investigation project of the shale gas and oil potential was carried out by Ministry of Land and Resource of China. This work was part of this endeavor.

In this study, a detail shale gas evaluation was carried out on the Badaowan shale combined with well drilling geological survey and petrological, petrophysical and geochemical laboratory tests. In addition, TOC content of shale interval was calculated based on measured TOC and logging data. Then a three-dimensional (3D) model was built to exhibit the spatial distribution of the Badaowan shale gas prospect in the Junggar basin. The objective of this work is to provide a general methodology that is applicable for investigating shale gas potential in other gas bearing basins.

2. Evaluation Criteria and Method of Shale Gas Prospect Identification in this Study

2.1 Evaluation Criteria

Numerous studies about defining shale gas prospect of the successful shale gas plays had been conducted. The TOC content, thickness, organic matter (OM) type, thermal maturity, depth and mineral composition [2,3,8,9,11,24,30] were widely recognized as the main factors to determine a shale gas prospect and were always used as key parameters in assessment of shale gas resources. As the lack of mineral composition data, key parameters used for prospect identification in this study included TOC content, thickness, OM type, thermal maturity and depth.

Evaluation criteria for shale gas prospects in continental deposit was applied in this study, which was published by Research Center of Oil and Gas Resources (RCOGR) of Ministry of Land and Resource of China [31] (Table 1).

Table 1. Evaluation criteria for shale gas prospects in continental deposits

Key Parameter	Criterion
Thickness of shale	Net shale≥10m or gross shale interval≥30m with the proportion of shale that is ≥60%
TOC	≥1.5%
R_o	For Type I, R_o≥1.2%; for type II, R_o≥0.7%; and for type III, R_o≥0.5%
Depth	300 ～ 4500m

DOI: https://doi.org/10.30564/jgr.v1i3.1385

2.2 Method of Prospect Identification

3D model has been used to evaluate shale gas potential in previous studies. For example, a 3D high-resolution model was utilized to assess the shale gas potential in Germany and Netherland [32-34]. Wang and Carr [35] utilized core analysis data, log data and seismic data to construct a 3D shale lithofacies of Marcellus Shale in Appalachian Basin of USA to identify the geologic and engineering sweet spots for gas production.

In this study, we improved the traditional method used for shale gas prospects identification from two-dimensional (planar) contour map inspection to three-dimensional investigation. By identifying the prospective shale intervals in wells according to the criteria (Table 1), a 3D model showing horizontal and vertical distribution of potential gas shales can be developed, which can result in a precise gas in place (GIP) assessment. Firstly, the TOC content of the shale intervals were calculated using logging data based on the measured TOC content. According to the criteria, minimum R_o are different for type I, type II and type III OM, and the OM type was identified using Rock-Eval pyrolysis data (TOC vs. S_2) in this study. Thermal maturity always increased with the burial depth, and the relationship between R_o and depth in different regions could be determined. The depth that corresponds to the minimum R_o cut-off was the minimum depth required for the prospect. That was, OM buried deeper than the minimum depth was considered mature and prospective. In addition, the portion with depth more than 4500 m was excluded due to economic feasibility according to the evaluation criteria of RCOGR. After that, the prospective shale intervals in wells were defined within the prospective range of depth to ensure that they satisfied the thickness and TOC content requirements at the same time (Figure 1). Lateral continuity was taken into consideration in a spatial distribution as well. Finally, the prospect was delineated as a 3D model based on the continuous distribution of the prospective shale intervals.

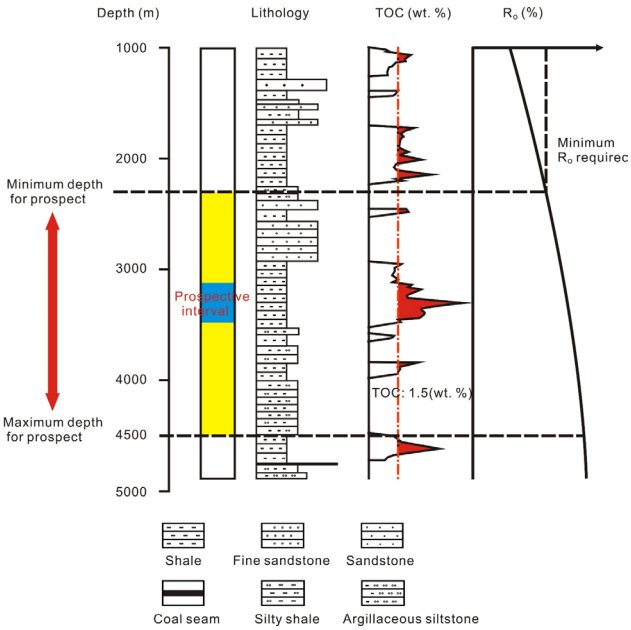

Figure 1. Workflow to identify the prospective intervals

3. Geological Setting

Junggar Basin, with an area of 13×10^4 km^2, was one of the most important oil and natural gas provinces in China [36-68]. Junggar Basin was an upper Paleozoic, Mesozoic, and Cenozoic basin superimposed at the junction of the Kazakstan block, the Siberia block, and the Tarim block [39]. The tectonic and lithostratigraphic units of the Junggar basin can be generally subdivided into four megasequences [40]: (1) foreland oceanic basin stage (Pennsylvanian–Lower Permian), (2) foreland continental basin stage (middle–Upper Permian), (3) intracontinental depression stage (Triassic–Cretaceous), and (4) rejuvenated foreland basin stage (Paleogene–Quaternary). The Junggar Basin can be divided into the following six first-order tectonic units: Wulungu Depression in the north, West Uplift in the west, East Uplift in the east, Southern Depression in the south, and Luliang Uplift and Central Depression in the center (Figure 2).

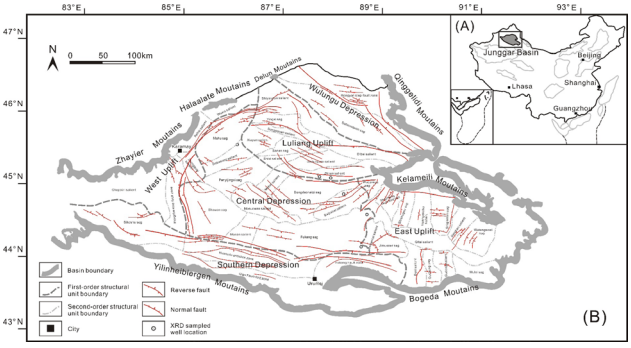

Figure 2. Location map (A) and structural features (B) of Junggar Basin

The natural gas in Junggar Basin mainly originated from Carboniferous, Jurassic and Permian strata (Figure 3) [41-43]. In particular, the middle and lower parts of Jurassic strata were the predominant gas source rocks [29,44,45]. Badaowan Formation, the lowest unit of Jurassic strata, was organic-rich shale which was widely distributed spatially with suitable thickness [29,46].

DOI: https://doi.org/10.30564/jgr.v1i3.1385

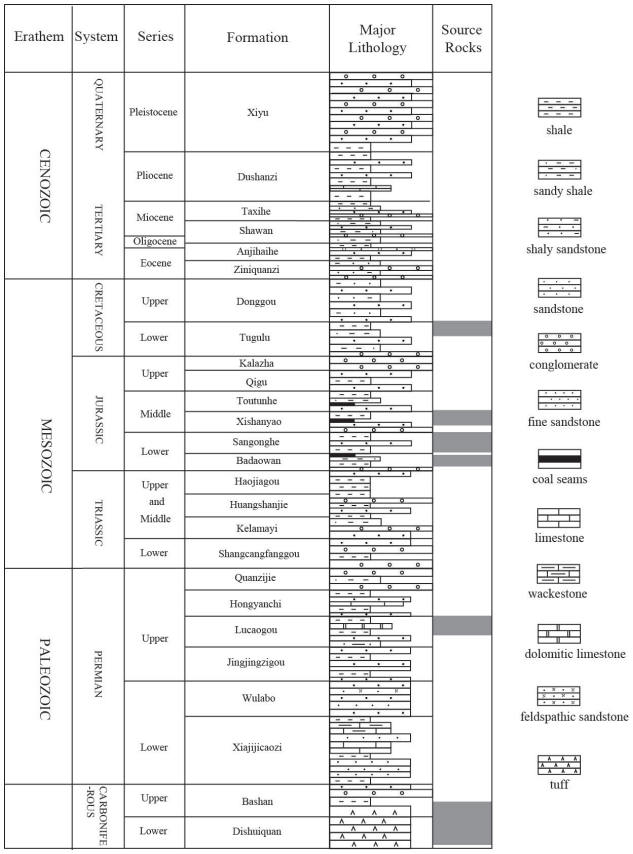

Figure 3. Stratigraphic column and natural gas source rocks in Junggar Basin

4. Samples and Methods

4.1 Database and Samples

Rock-Eval pyrolysis data (S_1, S_2 and T_{max}) and vitrinite reflectance (R_o%) of 284 shale samples from 23 wells for lab analysis and well information (lithology and logging data) of 67 wells for prospects identification were provided by Xinjiang Oil Field Company, PetroChina.

4.2 Experimental Methods

X-ray diffraction (XRD) was performed on nine samples to identify the mineral composition. The experimental temperature and humidity was 24 ºC and 35%, respectively. Crushed samples (< 200 μm) were mixed with ethanol first, and then handground and smear mounted on glass slides for X-ray diffraction analysis. The measurements were performed using a Bruker D8-Discover Advance X-ray Diffractometer with Co Kα-radiation produced radiation (45 kV, 35 mA) over an angular range of 2-60º(2θ) at scan rates of 2º/min (2θ). Quantitative phase analysis was performed by Rietveld refinement, with customized clay mineral structure models [47].

Parallel samples of Rock-Eval pyrolysis were pulverized to 200 mesh in preparation for TOC measurement. TOC contents of these core samples were determined using a LECOCS-400 analyzer (LECO Corp., USA). Methane adsorption isotherms were also applied to analyze the gas sorption capacity of prospective interval of the Badaowan shale. The isotherms were performed on FY–KT1000 isothermal adsorption apparatus. Methane (purity 99.999%) was used as adsorbate gas. The experimental pressures (from 0 to10.8 MPa) were measured and seven volume points corresponding to the pressures were recorded. The gas adsorption capacity was calculated using the Langmuir model as

$$V = V_L P/(P_L+P),$$

where V was the volume of absorbed gas; V_L was the Langmuir volume (based on monolayer adsorption), which is the maximum adsorption capacity at complete surface coverage; P was the gas pressure; P_L was the Langmuir pressure, at which the absorbed gas content (V) was equal to half of the Langmuir volume (V_L) [48].

TOC measurement was performed at State Key Laboratory of Petroleum Resources and Prospecting, China University of Petroleum (Beijing).All the remain experiments were performed at Bangda New Technology Co. Ltd., Renqiu, China.

4.3 TOC Content Calculation

To identify a prospective interval, continuous TOC content of each shale interval was required. The relationship between the measured TOC content and resistivity logging and acoustic time could be established to calculate the TOC content of shale interval without measurement [49].

$\Delta log\ R = \log(R/R_{baseline}) + 0.02 \times (\Delta t - \Delta t_{baseline})$, where $\Delta log\ R$ was the curve separation measured in logarithmic resistivity cycles; R was the resistivity measured in ohm-m by logging tool; Δt was the measured acoustic time in μs/ft; $R_{baseline}$ was the resistivity corresponding to the $\Delta t_{baseline}$ value when the curves were baselined in non-source rocks, and 0.02 was based on the ration of -50 μs/ft per one resistivity cycle mentioned above. Then one can fit a linear relationship between TOC and $\Delta log\ R$ to build an equation for TOC as $TOC_{measured} = a \times \Delta logR + b$, where a and b were parameters to be determined and their values could be determined using the measured TOC content and logging data.

5. Results and Discussion

5.1 Geochemical Characteristics

5.1.1 OM Richness

TOC content ranged from 0.05 to 8.18 wt. % with an

 DOI: https://doi.org/10.30564/jgr.v1i3.1385

average of 1.30 wt. %. S_1+S_2 ranged between 0.06 to 24.82 mg/g with an average of 2.31 mg/g. In the northwestern margin, the TOC content and S_1+S_2 ranged from 0.14 to 8.18 wt. % and from 0.17 to 21.39 mg/g, respectively while the average TOC content and S_1+S_2 were 1.32 wt. % and 1.50 mg/g, respectively (Figure4). The TOC content and S_1+S_2 in the Luliang Uplift averaged 1.05 wt. % and 3.05 mg/g, respectively (Figure4). The average values of TOC content and S_1+S_2 in Wulungu Depression were 1.38 wt. % and 3.24 mg/g, while they were 1.76 wt. % and 4.08 mg/g in the eastern Central Depression, respectively. Guo et al. [29] reported that in the southern Junggar Basin, the TOC content of the Badaowan shale ranged from 0.13% to 5.77 wt. % and averaged 1.69 wt.% with 65.8% of the 225 samples exceeding 1 wt.% TOC content, and the average S_1+S_2 was 2.29 mg/g. By comparison, it showed no obvious difference among different first-order tectonic units on the TOC content and genetic potential (S_1+S_2).

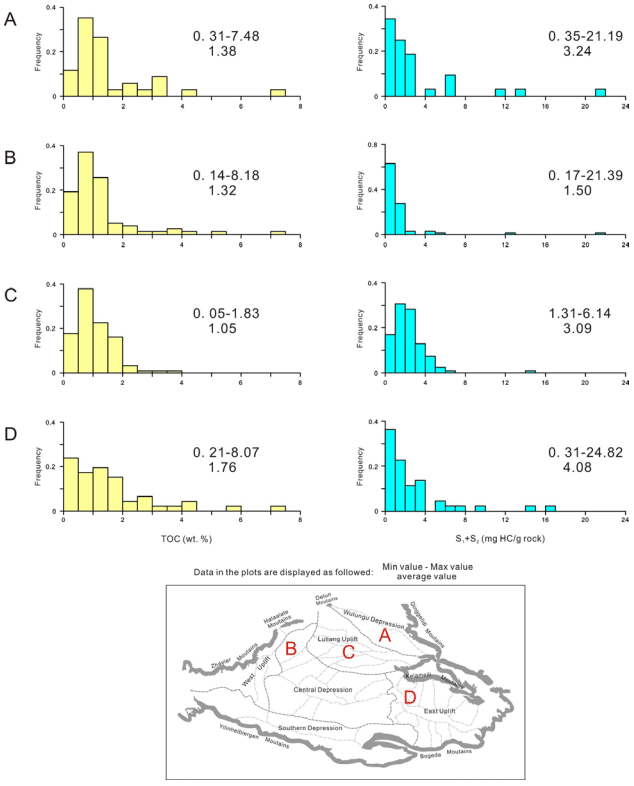

Figure 4. TOC content (yellow) and S_1+S_2 (green) histograms of the Badaowan shale in different first-order structural units

5.1.2 OM Type

Plots of S_2 versus TOC were used to identify the OM type of the Badaowan shale. Figure5 shows that type III OM dominated most of the northern Junggar Basin (Figure 4). Similarly, OM in the southern basin was dominated by type III with small amounts of type II and type I [29,50,51].

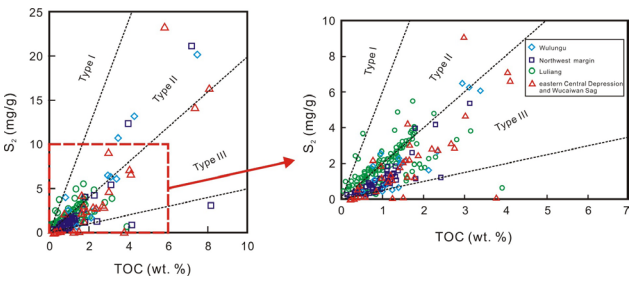

Figure 5. S_2 versus TOC content to identify the OM type for the Badaowan shale

5.1.3 Thermal Maturity

The measured R_o ranges from a minimum of 0.47% at 2900 m in the eastern Central Depression, to 0.81% at 3781 m in the Wulungu Depression, and most R_o values were greater than 0.5% (Figure 6A). Guo et al. [29] reported that most R_o obtained from the Badaowan shale in southern basin ranged between 0.5% and 1.3% while T_{max} values ranged from 425 to 465 °C. The Badaowan shale reached over-mature at deeper sites in the southern basin. In most area of the Eastern Uplift, R_o was lower than 0.4% at present (Figure 7) [52], therefore this region did not have favorable geochemical conditions for shale gas reserves.

R_o was correlated with depth to identify the depth at which R_o is 0.5% (minimum R_o cut-off for type III OM), and this depth value was used in the identification. In the northwestern margin of Junggar Basin, a relatively good correlation between R_o and depth existed. It showed that the depth at which R_o of 0.5% was approximately 2230 m (Figure 6C) while 2920 m in the Luliang Uplift (Figure 6D). The corresponding depths in the Wulungu Depression and eastern Central Depression (including Wucaiwan Sag) were 1560 m (Figure 6B) and 2310 m (Figure 6E), respectively.

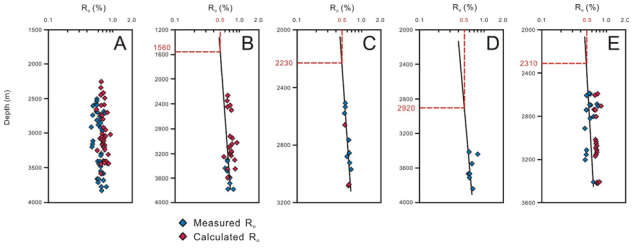

Figure 6. R_o versus depth for the Badaowan shale in different structural units. Calculated R_o =0.018×T_{max}-7.16 [53], with T_{max} less than 420℃ or higher than 500℃, and T_{max} with S_2 lower than 0.5 mg/g was not calculated [54]

Note: A: entire Badaowan shale; B: Wulungu Depression; C: northwestern margin; D: Luliang Uplift; E: eastern Central Depression and Wucaiwan Sag.

DOI: https://doi.org/10.30564/jgr.v1i3.1385

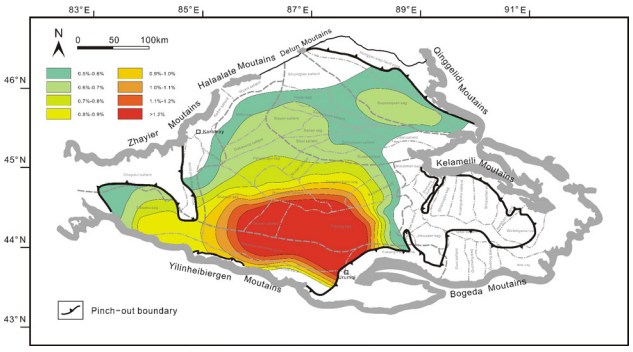

Figure 7. A contour map of the vitrinite reflectance at the top of the Badaowan Formation in the Junggar Basin

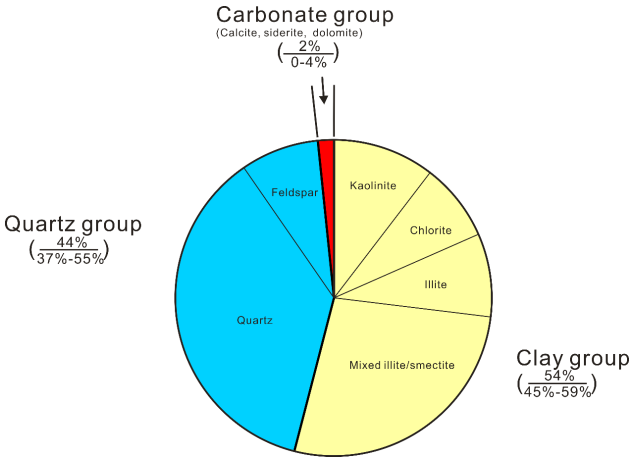

Figure 8. Mineral composition of the Badaowan shale; upper value indicated the average value of the composition, bottom values indicated the range of the composition.

5.2 Mineral Composition

Generally, mineral composition can be divided into three groups, quartz group (quartz, feldspar and pyrite), carbonate group (calcite, dolomite and siderite), and clay group (kaolinite, chlorite, illite, smectite and I/S) [55]. The results of X-ray diffraction (XRD) analyses showed that clay minerals (kaolinite, chlorite, illite and mixed layers illite-smectite) were the primary components in the Badaowan shale, which represented 54% of the bulk mineral content (Table 2, Figure 8). Generally, the clay minerals primarily consisted of illite and mixed illite/smectite. Quartz-related minerals ranged between 37% and 55% with an average of 44% of the bulk mineral content. There was also a minor amount of carbonate (calcite, dolomite, and siderite) minerals (less than 5%).

5.3 Distribution and Burial Depth

The Badaowan shale was mainly distributed in the eastern Wulungu Depression, Central Depression and Southern Depression. Its thickness increased from north to south, and reached over 400 m in the Southern Depression (Figure 9) [29,46]. In the most part of the Eastern Uplift, the development of the Badaowan shale was less. The burial depth of the Badaowan shale increased from north to south ranging from approximately 1000 m to 9000 m. In the most part of Central Depression and Southern Depres-

Table 2. The mineral composition of the Badaowan shale

Well ID	Sample ID	Depth (m)	K	C	I	I/S	%S	Clay	Quartz	KF.	PL.	Cal.	Sid.	Dol.
DX3	YQ44	3137.88	15	15	20	50	25	59	34	/	4	3	/	/
D9	YQ30	3534.51	20	12	13	55	25	56	34	/	10	/	/	/
F1	YQ35	3205	9	13	22	56	25	50	39	/	8	/	3	/
F1	YQ34	3133.6	8	10	14	68	30	45	43	1	11	/	/	/
D9	YQ43	3534.88	20	16	12	52	20	58	34	/	8	/	/	/
DX2	YQ46	3374.76	16	14	16	54	20	59	29	/	8	/	4	/
C16	YQ45	2831	41	16	18	25	20	57	39	2	2	/	/	/
B13	YQ29	2863.58	35	22	8	35	50	53	39	/	8	/	/	/
F1	YQ38	3200	10	14	19	57	25	49	37	/	10	/	/	4

Note: In the table, K=kaolinite, C=chlorite, I=illite, I/S= mixed layers illite-smectite; these content referred to the proportion of the total clay minerals. KF.=K-feldspar, PL.=plagioclase, Cal.=calcite, Sid.=siderite, Py. =pyrite and Dol.=dolomite.

 DOI: https://doi.org/10.30564/jgr.v1i3.1385

sion, where the Badaowan shale was well developed, the burial depth was over 5000 m (Figure 10) [46]. A considerable thickness of organic-rich shale in gas window was deposited in Central Depression and Southern Depression [29], however, reduced physical properties (porosity and permeability) and high drilling costs due to the burial depth made the shale gas exploitation unfeasible at present.

Therefore, a potential area for shale gas prospect was identified and mapped in Figure11, and was delineated by red dashed line based on the geological and geochemical characteristics discussed above. In Eastern Uplift, the Badaowan shale was not well developed, and the thermal maturity was at a relatively low level. In the Southern Depression and the most part of Central Depression, the maximum burial depth of the Badaowan Formation was deeper than 5000 m, which cannot be explored and developed economically. Therefore, these two regions were not favorable for shale gas exploitation. 67 wells distributed throughout the potential prospect area were used for identifying shale gas prospect (Figure 11).

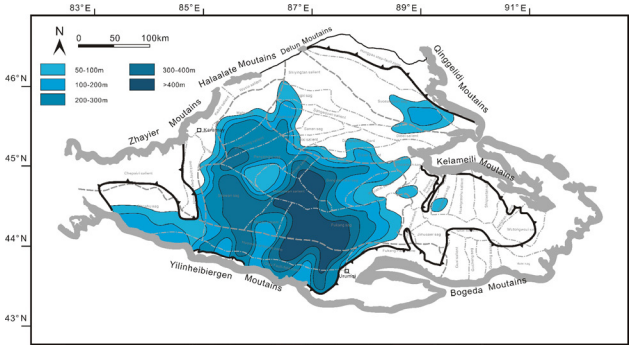

Figure 9. A contour map showing the horizontal distribution of the Badaowan shale

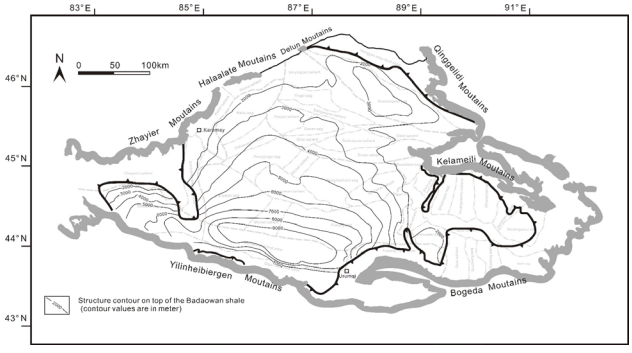

Figure 10. A map showing the structure contour on the Badaowan shale

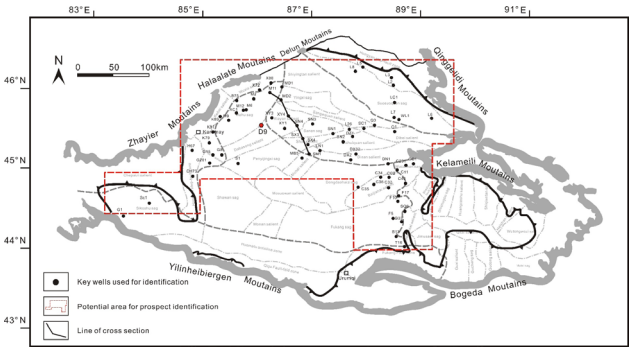

Figure 11. A map showing the potential area for shale gas prospect and key wells used for identification

5.4 Prospect Identification

Shale gas prospect was identified according to the distribution of the prospective intervals in wells. By identifying the prospective intervals in wells, a spatial prospect model could be developed and the prospects can be delineated. Finally, the prospect was delineated as a 3D model based on the continuous distribution of the prospective shale intervals (Figure 12).

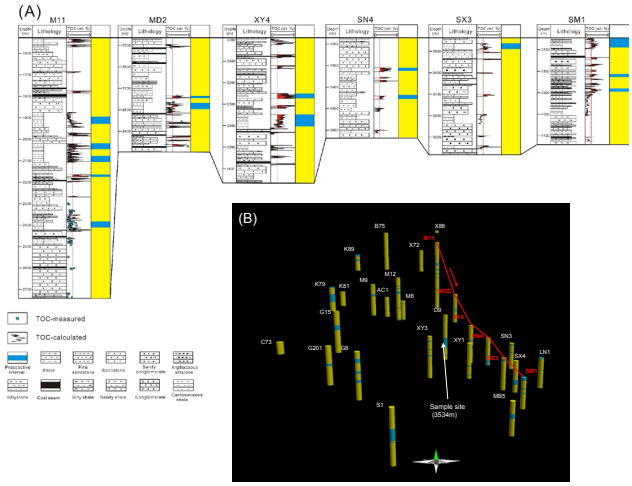

Figure 12. Prospective intervals identification in wells (A) and their spatial distribution (B)

Note: In the well correlation, blue circles represented measured TOC content and black curves represented calculated values; prospective intervals were marked by blue. In plot (B), site of the core sample used for methane sorption experiment was shown. Location of cross section and D9 Well are shown in Figure 11.

Three shale gas prospects were defined (Figure 13A-D): (1) the largest shale gas prospect covered an area of over 15900 km^2 from the northwest Central Depression to the west Luliang Uplift (Figure13B). Within this prospect, there were three main favorable intervals that were distributed with a high level of lateral continuity. The upper prospective interval was

DOI: https://doi.org/10.30564/jgr.v1i3.1385

mainly distributed in the Mahu Sag and Dabasong Uplift have a maximum thickness of 40m. The burial depth of the upper interval ranged from 2250 m to 3200 m and increased from the Mahu Sag towards the southwest direction. Within the upper prospective interval, a thin interlayer of coal also presented. The middle two prospective intervals have a good horizontal continuity and distributed throughout the prospect with a maximum thickness of 200 m. The depth of the two middle intervals ranged from 2300 m to 4420 m and increased obviously from Kebai Salient to the south. R_o of prospective intervals in this prospect ranged from 0.5% to 0.75% approximately (predicted from the correlation between R_o and depth) (2) The Wulungu prospect was located at the foot of the Qinggelidi Mountains with an area of 4474 km^2 (Figure13C). Burial depth of prospective intervals ranged between 1960 m and 3640 m, and R_o of which ranged from 0.6% to 0.9% approximately. Based on the wells identified in the Wulungu Depression, the prospective shale interval was mainly on the middle part of the Badaowan Formation with the thickness ranging from 12 m to 110 m which thinned from east to west and deepened from east at the foot of the mountains to west. The shale proportion of the intervals was over 90% and thin interlayers within the interval were mainly argillaceous siltstone and coal seam. However, the prospect may not be reliable enough compared with the other two prospects because few wells had been drilled in the Wulungu Depression, and only eight wells were used to identify the prospect in this study. (3) The shale gas prospect in the eastern Central Depression extended over an area of 4500 km^2 (Figure13D). Depth of the favorable shale intervals ranged from 2400m to 3400m, and the thickness of prospective interval ranged from 10 m to 75 m interbedded with thin layers of sandy mudstone, fine sandstone and argillaceous siltstone. R_o of prospective intervals ranged from 0.5% to 0.7% approximately.

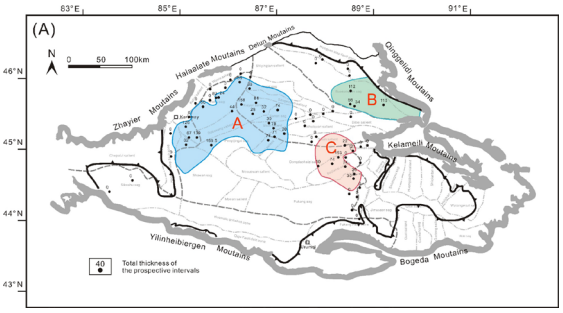

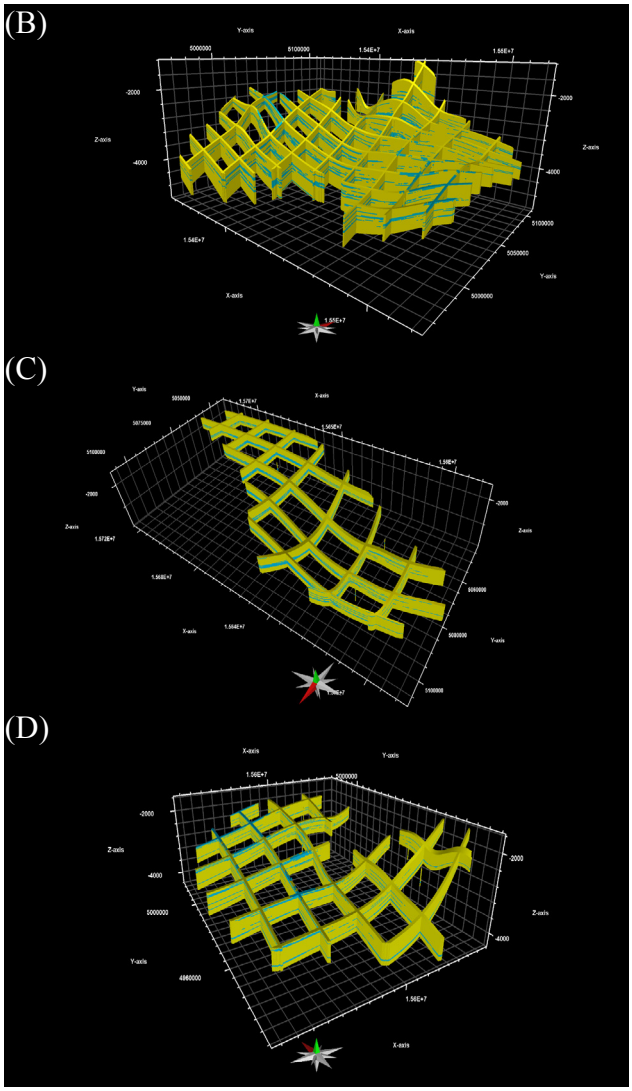

Figure 13. (A)The distribution of the identified shale gas prospects for the Badaowan shale. (B), (C) and (D) showed the fence diagrams for the three prospects. (B) Prospect in the northwest Central Depression to the west Luliang Uplift. (C) Prospect in the Wulungu Depression. (D) Prospect in the eastern Central Depression

5.5 Gas Capacity

To verify the gas capacity of shales within the prospects, methane sorption experiment was carried out. Methane sorption volumes at different temperatures from samples in prospective interval of northwest margin were measured (sampled well were shown in Figure 11). The results showed that maximum methane sorption capacity varied from 0.72 m^3/t at 70 ºC to 1.62 m^3/tat 30 ºC (Table 3), and decreased with increasing temperature. As shown in Figure 14A, the shape of isotherms changed with temperature. Methane sorption capacity rose with increasing pressure and became constant at 5 MPa approximately at 70 ºC.

DOI: https://doi.org/10.30564/jgr.v1i3.1385

Many studies had showed that TOC content have a significant effect on methane sorption capacity and there was a relatively nice linear correlation between TOC content and methane sorption capacity [3,8,9,56]. Generally, methane sorption capacity of the Badaowan shale was comparable to other typical gas shales from different geological ages with similar TOC contents (Figure 14B). The measured samples in this study fitted the trend between TOC content and methane sorption capacity.

Table 3. Measured methane sorption capacity for a sample of D9 well

YQ 30, TOC = 1.32 wt. %					
70 °C		50 °C		30 °C	
P (MPa)	CH_4 (m^3/t rock)	P (MPa)	CH_4 (m^3/t rock)	P (MPa)	CH_4 (m^3/t) rock)
0	0	0	0	0	0
0.38	0.13	0.35	0.16	0.37	0.13
1.04	0.27	1	0.45	1.03	0.37
2.21	0.48	2.26	0.82	2.24	0.64
4.28	0.56	4.33	1.25	4.31	0.85
6.21	0.58	6.27	1.38	6.24	1
8.67	0.66	8.74	1.54	8.62	1.09
10.83	0.72	10.85	1.62	10.85	1.22

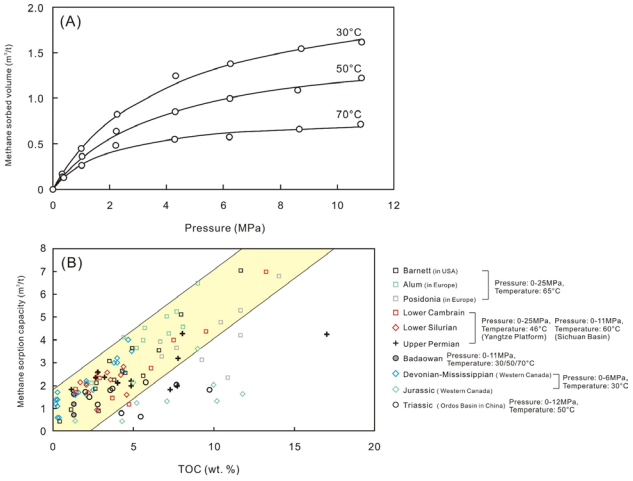

Figure 14. (A) The methane sorption isotherms of core sample from prospective interval on D9 Well within the prospect A. Points reflected measured value about adsorbed methane amount, and lines were calculated adsorbed methane based on the Langmuir model. (B) Comparison of methane sorption capacity of the Badaowan shale and some typical gas shales in China, United States and Canada [10,56-59].

Note: Experimental conditions (pressure and temperature) for gas shales are shown in the plot. Location of D9 Well is shown in Figure 11.

6. Conclusions

The following conclusions can be drawn from this study.

(1) The measured TOC content of the Badaowan shale ranged from 0.05 to 8.18 wt.% with an average value of 1.30wt.%. The OM was dominated by gas-prone type III. The measured R_o ranged from 0.47% to 0.81%. The Badaowan shale was mainly distributed in the eastern Wulungu Depression, Central Depression and Southern Depression. The burial depth of the Badaowan shale ranged from approximately 1000 m to 9000 m and increased from north to south. In most of Central Depression and Southern Depression, where the Badaowan shale was well developed, burial depth was over 5000 m. The Badaowan shale showed a high homogeneity in mineral composition with a high content of clay minerals (average of 54%) and quartz related minerals (average of 40%).

(2) Based on geochemical, geological and well logging analysis of the Badaowan shale, prospective intervals of wells were selected and a 3D model was built to delineate the shale gas prospects. Three shale gas prospects were identified: (1) northwestern margin-west Luliang prospect, Wulungu prospect and eastern Central Depression prospect. Compared with the other two prospects, the one located in the northwestern Central Depression-west Luliang Uplift had an area of 15900 km^2 and shale intervals with a high lateral continuity, therefore it was considered to have a significant potential of shale gas resource worthy of future exploration and development. In particular, the middle intervals, which were distributed throughout the prospect, should be considered as the most favorable exploration target. Within the northwestern margin-west Luliang prospect, samples from the prospective were utilized to investigate the gas capacity. The methane sorption capacity of the Badaowan shale decreased as the experimental temperature increasing, and it was comparable to that of typical gas shales worldwide.

Through the comprehensive method, vertical and horizontal distribution of prospective shales can be observed directly in comparison with traditional method. Application of this method in petroliferous basins with high exploration and development degree, a more precise model could be obtained since larger numbers of wells and analyzed data could be involved into prediction. It is hoped that this study can provide a helpful workflow to evaluate shale gas potential, in particular in a basin scale.

Nomenclature

BBO = billion (10^9) barrels of oil.

HI = hydrogen index, S_2 divided by TOC×100 (mg HC/g TOC).

DOI: https://doi.org/10.30564/jgr.v1i3.1385

OM =organic matter.

R_o = vitrinite reflectance (%).

S_1 = free hydrocarbons present in the rock (mg/g).

S_2 = petroleum generated by pyrolysis (mg/g).

S_1+S_2 = genetic potential (mg/g).

T_{max} = the temperature at peak evolution of S_2 hydrocarbons(℃).

Tcf = trillion (10^{12}) cubic feet.

TOC = total organic carbon (wt.%).

XRD= X-ray diffraction

Acknowledgements

This work was supported by the special program (Grant No. 2009GYXQ15-09-03) of shale gas potential assessment and selection of favorable exploration areas in China of the Research Center of Oil and Gas Resources of the Ministry of Land and Resources.

References

[1] EIA. International Energy Outlook 2016, US Department of Energy/EIA, Washington, DC, 2016.

[2] Curtis J.B.. Fractured shale-gas systems, AAPG Bull., 2002, 86(11): 1921-1938.

[3] Hao, F., Zou, H.Y. Lu, Y.. Mechanisms of shale gas storage: Implications for shale gas exploration in China, AAPG Bull., 2013, 97(8): 1325-1346.

[4] Horsfield, B. Schulz, H.M.. Shale gas exploration and exploitation, Mar. Petrol. Geol., 2012, 31: 1-2.

[5] Kou, R., Alafnan, S.F.K. and Akkutlu, I.Y.. Multiscale Analysis of Gas Transport Mechanisms in Kerogen, Transport Porous Med., 2016, 116: 493-519.

[5] Zhang, Z.H., Xiang, K., Qing, L.M., Zhuang, W.S., Xi, W.J. and Zhao, S.F.. Geochemical characteristics of source rocks and their contribution to petroleum accumulation of Chepaizi area in Sikeshu depression, Junggar Basin, Geol. China, 2012, 39(2): 326-337 (in Chinese with English abstract).

[6] Sun, J.L., Gamboa, E.S., Schechter, D. and Rui, Z.H.. An integrated workflow for characterization and simulation of complex fracture networks utilizing microseismic and horizontal core data, J. Nat. Gas Sci. Eng., 2016, 34: 1347-1360.

[7] Sun, J.L., Zou, A., Sotelo, E. and Schechter, D.. Numerical simulation of CO2 huff-n-puff in complex fracture networks of unconventional liquid reservoirs, J. Nat. Gas Sci. Eng., 2016, 31: 481-492.

[8] Ross, D. and Bustin. R.M.. Shale gas potential of the lower Jurassic Gordondale member, northeastern British Columbia, Canada, Bull. Can. Petrol. Geol., 2007, 55(1): 51-75.

[9] Ross, D. and Bustin. R.M.. Characterizing the shale gas resource potential of Devonian–Mississippian strata in the Western Canada sedimentary basin: Application of an integrated formation evaluation, AAPG Bull., 2008, 92(1): 87-125.

[10] Ross, D.J. and Bustin, R.M.. The importance of shale composition and pore structure upon gas storage potential of shale gas reservoirs, Mar. Petrol. Geol., 2009, 26: 916–927.

[11] EIA.. Technically Recoverable Shale Oil and Shale Gas Resources: An Assessment of 137 Shale Formations in 41 Countries Outside the United States. US Department of Energy/EIA, Washington, DC, 2013.

[12] Pollastro, R.M., Jarvie, D.M., Hill, R.J. and Adams, C.W.. Geologic framework of the Mississippian Barnett Shale, Barnett-Paleozoic total petroleum system, Bend arch-Fort Worth Basin, Texas, AAPG Bull., 2007, 91(4): 405-436.

[13] Rawsthorn, K.. Shale Gas Prospectivity Potential Prepared for: Australian Council of Learned Academies (Acola), Australian Council of Learned Academies (Acola), 2013.

[14] Chen, S.B., Zhu, Y.M., Qin, Y., Wang, H.Y., Liu, H.L. and Fang, J.H.. Reservoir evaluation of the Lower Silurian Longmaxi Formation shale gas in the southern Sichuan Basin of China, Mar. Petrol. Geol., 2014, 57: 619-630.

[15] Yan, J.F., Men, P.Y., Sun, Y.Y., Qian, Y., Liu, W., Zhang, H.Q., Liu, J., Kang, J.W., Zhang, S.N., Bai, H.H. and Zheng, X.. Geochemical and geological characteristics of the Lower Cambrian shales in the middle-upper Yangtze area of South China and their implication for the shale gas exploration, Mar. Petrol. Geol., 2016, 70: 1-13.

[16] Huang, J.L., Zou, C.N., Li, J.Z., Dong, D.Z., Wang, S.J., Wang, S.Q., Wang, Y.M., Li. D.H.. Shale gas accumulation conditions and favorable zones of Silurian Longmaxi Formation in south Sichuan Basin, China, J. China Coal Soc., 2012, 37(5): 782-787.

[17] Long, P.Y., Zhang, J.C., Li, Y.X., Tang, X., Cheng, L.J., Liu, Z.J., Han, S.B.. Reservoir-forming conditions and strategic select favorable area of shale gas in the Lower Paleozoic of Chongqing and its adjacent areas. Earth Science Frontiers.,2012, 19(2): 221-243 (in Chinese with an English abstract).

[18] Nie, H.K., Tang, X., Bian, R.K.. Controlling factors for shale gas accumulation and prediction of potential development area in shale gas reservoir of South China. Acta Petrolei Sinica., 2009, 30(4): 484-491(in Chinese with an English abstract).

[19] Pu, B.L., Jiang, Y.L., Wang, Y., Bao, S.J. Liu, X.J.. Reservoir forming conditions and favorable exploration zones of shale gas in Lower Silurian Longmaxi

 DOI: https://doi.org/10.30564/jgr.v1i3.1385

Formation of Sichuan Basin. Acta Petrolei Sinica, 2010, 31(2): 225-230 (in Chinese with an English abstract).

[20] Shan, Y.S., Zhang, J.C., Li, X.G., Wang, L. Ge, M.N.. Shale gas accumulation factors and prediction of favorable area of Taiyuan Formation in Liaohe Eastern Up-lift. J. Daqing Petrol. Inst., 2012, 36(1): 1-7 (in Chinese with an English abstract).

[21] Bohacs, K.M.. Contrasting Expressions of Depositional Sequences in Mudstones from Marine to Non-marine Environs, in Schieber, J., Zimmerle, W., and Sethi, P., eds., Mudstones and Shales, vol. 1, Characteristics at the Basin scale: Stuttgart, Schweizerbart'sche Verlagsbuchhandlung, 1998: 32–77.

[22] Bohacs, K.M., Grawbowski, G.J., Carroll, A.R., Mankeiwitz, P.J., Miskell-Gerhardt, K.J., Schwalbach, J. R., Wegner, M. B., Simo, J.A.. Production, Destruction, and Dilution – the Many Paths to Source-Rock Development, SEPM Special Publication 2005, 82: 61-101.

[23] Guthrie, J.M. and Bohacs, K.M.. Spatial Variability of Source Rocks: a Critical Element for Defining the Petroleum System of Pennsylvanian Carbonate Reservoirs of the Paradox Basin, SE Utah. in W.S. Houston, L.L. Wray, P.G.Moreland, eds., The Paradox Basin Revisited -- New Developments in Petroleum Systems and Basin Analysis, RMAG 2009 Special Publication -- the Paradox Basin, 2009: 95-130.

[24] Passey, Q.R., Bohacs, K.M., Esch, W.L., Klimentidis, R. Sinha, S.. From oil-prone source rock to gas-producing shale reservoir–geologic and petrophysical characterization of unconventional shale-gas reservoirs, Beijing, China, 2010.

[25] Jia, C.Z., Zheng, M., Zhang, Y.F.. Unconventional hydrocarbon resources in China and the prospect of exploration and development, Petrol. Explor. Dev., 2012, 39(2): 139–146.

[26] Jiang, F.J., Pang, X.Q. and Ouyang, X.C.. The main progress and problems of shale gas study and the potential prediction of shale gas exploration, Earth Sci. Front., 2012, 19: 198-211 (in Chinese with an English abstract).

[27] Stevens, S. H., Moodhe, K. D. Kuuskraa, V. A.. China Shale Gas and Shale Oil Resource Evaluation and Technical Challenges. In Society of Petroleum Engineers report 165832, presented at the Society of Petroleum Engineers Asia Pacific Oil and Gas Conference and Exhibition. Jakarta, Indonesia, 2013.

[28] Zou, C.N., Dong, D.Z., Yang, H., Wang, Y.M., H, J.L., Wang, S.F. and Fu, C.X.. Conditions of shale gas accumulation and exploration practices in China. Nat. Gas Ind., 2011, 31(12): 26-39 (in Chinese with English abstract).

[29] Guo, J.G., Pang, X.Q., Guo, F.T., Wang, X.L., Xiang, C.F., Jiang, F.J., Wang, P.W., Xu, J.,Hu, T. Peng, W.L.. Petroleum generation and expulsion characteristics of Lower and Middle Jurassic source rocks on the southern margin of Junggar Basin, northwest China: implications for unconventional gas potential, Can. J. Earth Sci., 2014, 51: 537-557.

[30] Boyer, C., Kieschnick, J., Suarez-Rivera, R., Lewis, R. E. and Waters, G.. Producing gas from its source, Oilfield Rev., 2006, 18: 36-49.

[31] Zhang, D.W., Zhang, J.C., Li, Y.X., Qiao, D.W. Jiang, W.L.. Shale gas assessment and selection of favorable exploration areas in China (in Chinese), Research Center of oil and Gas Resources of the Ministry of Land and Resources (RCOGR), 2012.

[32] Bruns, B., Littke, R., Gasparik, M., Van Wees, J.D., Nelskamp, S.. Thermal evolution and shale gas potential estimation of theWealden and Posidonia Shale in NW-Germanyand the Netherlands: a 3D basin modelling study, Basin Res., 2016, 28: 1-32.

[33] Mohnhoff, D., Littke, R. Sachse, V.F.. Estimates of shale gas contents in the Posidonia Shale and Wealden of the west central Lower Saxony Basin from high-resolution 3D numerical basin modelling, German J. Geol., 2016, 167(2/3): 295-314.

[34] Uffmann, K., Littke, R., Gensterblum, Y.. Paleozoic petroleum systems of the Munsterland Basin, Western Germany: a 3D basin modelling study-Part 2: Petroleum generation and storage with special emphasis on shale gas resource. Oil Gas European Magazine, 2014, 2/2014: 98-103.

[35] Wang, G. and Carr, T.R.. Methodology of organic-rich shale lithofacies identification and prediction: A case study from Marcellus Shale in the Appalachian basin, Comput. Geosci., 2012, 49: 151-163.

[36] Cao, J., Wang, X.L., Sun, P.A., Zhang, Y.Q., Tang, Y., Xiang, B.L., Lan, W.F. and Wu, M.. Geochemistry and origins of natural gases in the central Junggar Basin, northwest China, Org. Geochem., 2012, 53: 166–176.

[37] Shao, Y.. Petroleum accumulation of the Jurassic deeply-buried lower assemblage in the southern Junggar Basin. Geol. J. China Univ., 2013, 19(1): 86–94. (in Chinese with English abstract).

[38] Wang, X.L., Kuang, J. and Yang, H.B.. The Third-Round Assessment of Hydrocarbon Resources in the Junggar Basin. Internal Technical Report of Research Institute of Petroleum Exploration and Development, PetroChina Xinjiang Oilfield Company (in Chinese), 2000.

[39] Jin, Z.J., Cao, J., Hu, W.X., Zhang, Y.J., Yao, S.P.,

DOI: https://doi.org/10.30564/jgr.v1i3.1385

Wang, X.L., Zhang, Y.Q., Tang, Y. and Shi, X.P.. Episodic petroleum fluid migration in fault zones of the northwestern Junggar Basin(northwest China): Evidence from hydrocarbon-bearing zoned calcite cement, AAPG Bull., 2008, 92(9): 1225-1243.

[40] Chen, X., H. Lu, L. S. Shu, H. Wang, G. Zhang,., Study on tectonic evolution of Junggar Basin. Geol. J. China Univ., 2002, 8(3): 257–267 (in Chinese with English abstract).

[41] Li, P.L., Liu, C.H.. Exploration potential and migration-accumulation rules of natural gas in Junggar Basin, Acta Petrol. Sinica., 2005, 26(2): 6-10 (in Chinese with an English abstract).

[42] Yu, Y. J., Zhang, Y. J., Dong, D. Z. and Han, Y. K.. Current situation of natural gas exploration and its counter measures in Junggar Basin, Petrol. Explor. Dev., 2006, 33(3): 267-273 (in Chinese with an English abstract).

[43] Zhao, M.J., Song, Y., Liu, S.B., Yang, H.B., Liu, D.G.. Accumulation systems and filling process of natural gas in Junggar Basin. Geol. Rev., 2009, 55(2): 215-224 (in Chinese with an English abstract).

[44] Li, J., Jiang, Z.L., Xia, L., Wang, D.L., Han Z.X.. Geochemical characteristics of coal-measure source rocks and coal-derived gas in Junggar Basin, NW China, Petrol. Explor. Dev., 2009, 36(3): 365-374.

[45] Wu, X.Q., Huang, S.P., Liao, F.R., and Li, Z.S.. Geochemical characteristics and sources of natural gas from the south margin of Junggar Basin. Nat. Gas Geosci., 2009, 22(2): 224–232 (in Chinese with English abstract).

[46] Gao, J., Liu, G.D., Yang, W.W., Zhao, D.R., Chen, W., Liu, L.. Geological and geochemical characterization of lacustrine shale, a case study of Lower Jurassic Badaowan shale in the Junggar Basin, Northwest China, J. Nat. Gas Sci. Eng., 2016, 31: 15-27.

[47] Ufer, K., Stanjek, H., Roth, G., Dohrmann, R., Kleeberg, R., Kaufhold, S.. Quantitative phase analysis of bentonites by the Rietveld method. Clay. Clay Miner., 2008, 56(2): 272–282.

[48] Langmuir, I.. The adsorption of gases on plane surfaces of glass, mica and platinum, J. Am. Chem. Soc., 1918, 40: 1361–1403.

[49] Passey, Q.R., Creaney, S., Kulla, J.B., Moretti, F.J. and Stroud, J.D.. A practical model for organic richness from porosity and resistivity logs, AAPG Bull., 1990, 74(12): 1777-1794.

[50] Chen, J.P., Wang, X.L., Deng, C.P., Zhao, Z., Ni, Y.Y., Sun, Y.G., Yang, H.B., Wang, H.T., Liang, D.G., Zhu, R.K., Peng, X.L.. Geochemical features of source rocks in the southern margin, Junggar Basin, Northwestern China. Acta Petrol. Sinica, 2015, 36(11): 768-780 (in Chinese with an English abstract).

[52] Qiu, N,S., Zhang, Z,H. and Xu, E.S.. Geothermal regime and Jurassic source rock maturity of the Junggar Basin, northwest China, J. Asian Earth Sci., 2008, 31: 464-478.

[53] Jarvie, D.M. and Lundell, L.L.. Kerogen type and thermal transformation of organic matter in the Miocene Monterey Formation, In: Isaacs, C.M., Rullkötter, J. (Eds.),The Monterey Formation-from Rocks to Molecules, Columbia University Press, New York, 2001: 268-295.

[54] He, M., Graham, S., Scheirer, A. H. and Peters, K. E.. A basin modeling and organic geochemistry study in the Vallecitos syncline, San Joaquin Basin, California, Mar. Petrol. Geol., 2014, 49: 15-34.

[55] Tan, J.Q., Horsfield, B., Fink, R., Krooss, B., Schulz, H.M., Rybacki, E., Zhang, J.C., Boreham, C.J., Van Graas. G., Tocher, B. A.. Shale gas potential of the major marine shale formations in the Upper Yangtze Platform, South China, Part III: Mineralogical, lithofacial, petrophysical, and rock mechanical properties, Energ. Fuel., 2014, 28: 2322-2342.

[56] Tan, J.Q., Weniger, P.,Krooss, B., Merkel, A.,Horsfield, B., Zhang, J.C.,Boreham, C.J.,Van Graas. G., Tocher, B.A.. Shale gas potential of the major marine shale formations in the Upper Yangtze Platform, South China, Part II: Methane sorption capacity, Fuel, 2014, 129: 204-218.

[57] Gasparik, M.,Bertier, P.,Gensterblum, Y.,Ghanizadeh, A.,Krooss, B. M., Littke, R.. Geological controls on the methane storage capacity in organic-rich shales, Int. J. Coal Geol., 2014, 123: 34-51.

[58] Guo, H.J., Jia, W.L., Peng, P.A., Lei, Y.H., Luo, X.R., Cheng, M., Wang, X.Z., Zhang, L.X., Jiang, C.F.. The composition and its impact on the methane sorption of lacustrine shales from the Upper Triassic Yanchang Formation, Ordos Basin, China, Mar. Petrol. Geol., 2014, 57: 509-520.

[59] Wang, S.B., Song, Z.G., Cao, T.T., Song. X.. The methane sorption capacity of Paleozoic shales from the Sichuan Basin, China, Mar. Petrol. Geol., 2013, 44: 112-119.

 DOI: https://doi.org/10.30564/jgr.v1i3.1385